ELECTRICAL MODELING OF MAIN INJECTOR DIPOLE MAGNETS

Si. Fang

March 17, 1995

1. Introduction

The Main Injector Dipole ring consists of 344 dipole magnets with 216 six-meter dipoles and 128 four-meter dipoles. The ring is considered as a transmission line because the existence of capacitance between dipole magnet busses. In order to study the dipole ring transient response and obtain current regulation design information, the transmission line characteristics of the ring need to be understood. In this report, the electrical models for the dipole magnets are obtained by using five-terminal device measurement method. The models then are further simplified but yet keeping the electrical characteristics of the magnets for ring wide simulation.

2. Electrical Measurement

The dipole magnet is a five-terminal device. Fig 1 depicts the dipole magnet five-terminal device network. Terminal 1 and 3 represent the though bus. Terminal 2 and 4 represent the coil bus. Terminal 5 is the case ground of the magnet. The electrical characteristics of the magnet is described by its 5×5 admittance matrix at non-saturation. The equations for this five-terminal network can be written as

$$\begin{bmatrix} I_1 \\ I_2 \\ I_3 \\ I_4 \\ I_5 \end{bmatrix} = \begin{bmatrix} Y_{11} & Y_{12} & Y_{13} & Y_{14} & Y_{15} \\ Y_{21} & Y_{22} & Y_{23} & Y_{24} & Y_{25} \\ Y_{31} & Y_{32} & Y_{33} & Y_{34} & Y_{35} \\ Y_{41} & Y_{42} & Y_{43} & Y_{44} & Y_{45} \\ Y_{51} & Y_{52} & Y_{53} & Y_{54} & Y_{55} \end{bmatrix} \begin{bmatrix} V_1 \\ V_2 \\ V_3 \\ V_4 \\ V_5 \end{bmatrix} \qquad (1)$$

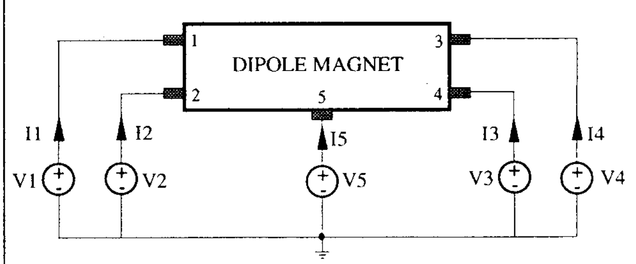

Fig 1. Dipole Magnet Five-Terminal Representation

Where

$Y_{ij} = \frac{I_i}{V_j}|_{V_k = 0, k \neq j, i = 1,2,3,4,5; j = 1,2,3,4,5; k = 1,2,3,4,5}$. The 5×5 matrix on the right hand side of Eqn. (1) is termed shorted circuit admittance matrix of the considered five-terminal dipole magnet device. The short circuit admittance matrix has a number of properties. One property of the admittance matrix derives directly from the cutset theory which constrains the sum of all terminal current to zero. Since

$$I_i = \sum_{j=1}^{5} Y_{ij} V_j \qquad (2)$$

$$\sum_{i=1}^{5} I_i = \sum_{i=1}^{5} \sum_{j=1}^{5} Y_{ij} V_j = 0 \qquad (3)$$

The right hand side of Eqn. (3) can be rewritten as

$$\sum_{j=1}^{5}\left(\sum_{i=1}^{5} Y_{ij}V_j\right) = 0 \tag{4}$$

and if this identity is to be valid for any and all V_j, it is clear that

$$\sum_{i=1}^{5} Y_{ij} = 0 \quad j = 1,2,3,4,5 \tag{5}$$

Eqn. (5) states that the sum of the elements appearing in any column of the shorted circuit admittance matrix is zero. A special case of Eqn. (4) is the situation in which all applied voltages are identical, that is $V_1=V_2=V_3=V_4=V_5=V$, then, in addition to the requirement that the sum of all current vanishes, the individual terminal currents must be zero since there is no potential difference exists across any terminal pair. Eqn. (2) collapses to

$$I_i = V\sum_{j=1}^{5} Y_{ij} = 0 \quad i = 1,2,3,4,5 \tag{6}$$

and the sum of the elements along any row is seen to be identical, In short, both column and row sums are zero for the admittance matrix.

The elements in the shorted circuit admittance matrix are frequency dependent variables. The way to measure this 5×5 matrix elements is depicts in figure 2. The excitation source used here is high power frequency generator (Elgar Model 500) that can output current up to 5 amps. the output voltage can be adjusted from 0 to 150 Vrms, and the frequency can be varied from 10 Hz to 10KHz. A Tektronix current probe, which has the bandwidth of DC to 50 MHz, was used for current measurement. Both voltage and current as well as phase shifted between voltage and current were measured by Tektronix scope. Ratio of peak to peak value of current to voltage was obtained for the shorted circuit admittance at particular frequency. Scope measurement for voltage and current makes sure the signals being measured are not distorted.

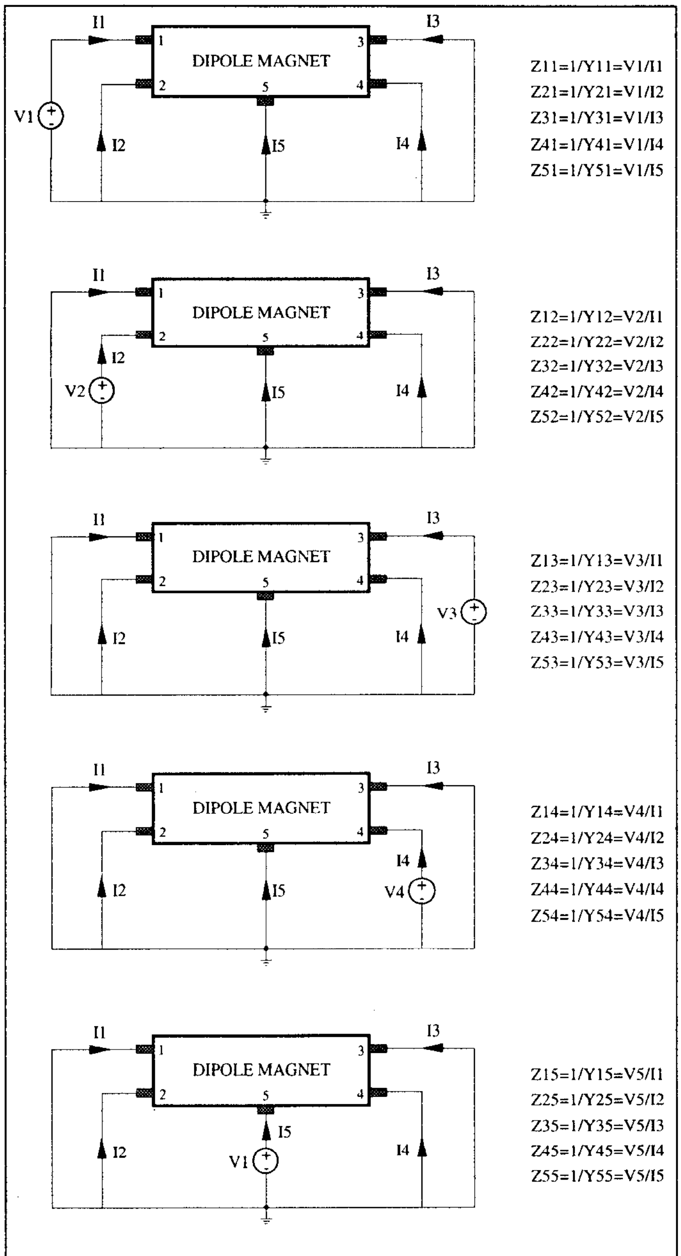

Fig 2. Admittance Matrix Measurement

The result of the shorted circuit impedance matrix elements (Z parameters) measurement are shown in appendix A-1 through appendix A-25 for 6 meter dipole magnet and appendix B-1 through appendix B-25 for 4 meter dipole magnet. Each of the measured shorted circuit impedance parameters is plotted in impedance magnitude and phase verses frequency in the range of 10 Hz to 10 KHz.

3. Electrical Models

It is difficult to guess a circuit such that this circuit fits all 25 matrix measurement data. In order to get the appropriate basic circuit configuration, we need to first start from the internal winding of dipole magnets.

3.1 Dipole Magnet Winding

The simplified internal winding of the dipole magnets is shown in figure 3. The through bus is the bus between terminal 1 and 3 with N1 represents 1/2 turn. The coil bus is the bus between terminal 2 and 4 with N7 represents 7 turns and N2 is the 1/2 turn. V3 is the voltage across the 7 turns and V2 is the voltage across the 1/2 turn as indicated in the drawing.

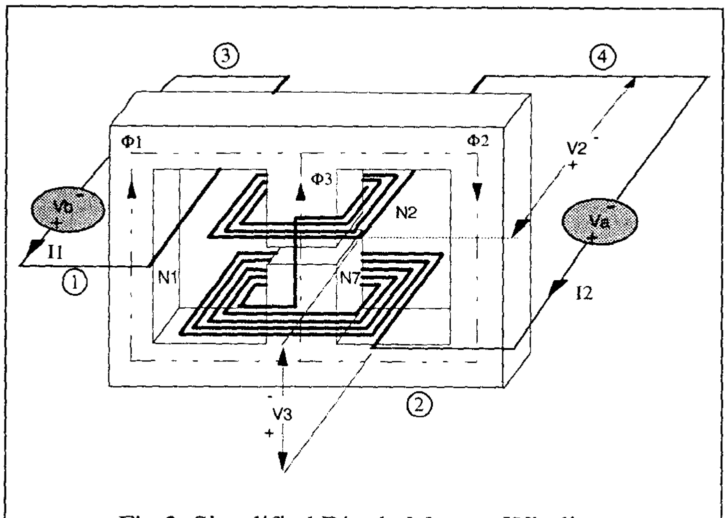

Fig 3. Simplified Dipole Magnet Winding

The magnetic circuit of dipole magnets can be represented by figure 4. The Rg is the reluctance of the air gap and Rc is the reluctance of the C core (Φ1 path) . The reluctance of air gap is much greater than the reluctance of the C core (Rg >> Rc). The flux Φ1, Φ2, Φ3 in the magnetic circuit can be solved and written as

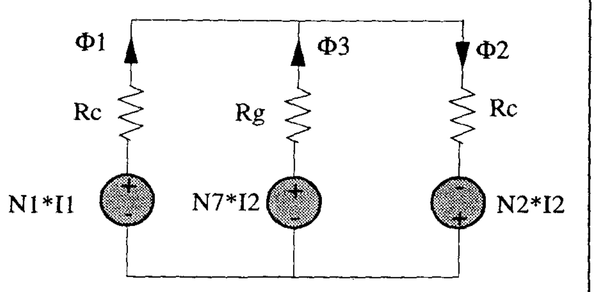

Fig 4. Dipole Magnet Magnetic Circuit

$$\Phi_1 = \frac{N_1 I_1 + N_2 I_2}{2R_c} + \frac{-N_7 I_2 + N_1 I_1}{2R_g} \tag{7}$$

$$\Phi_2 = \frac{N_2 I_2 + N_1 I_1}{2R_c} + \frac{N_7 I_2 + N_2 I_2}{2R_g} \tag{8}$$

$$\Phi_3 = \frac{N_7 I_2 - N_1 I_1}{2R_g} + \frac{N_7 I_2 + N_2 I_2}{2R_g} \tag{9}$$

Further evaluate Eqn. (7) to Eqn. (9) and use the relationship between flux and induced voltage, the governing equations for the magnetic circuit become

$$V_b = (\frac{N_1}{N_2})^2 L_c \frac{dI_1}{dt} + \frac{N_1}{N_2} L_c \frac{dI_2}{dt} - \frac{N_1}{N_7} L_g \frac{dI_2}{dt} + (\frac{N_1}{N_7})^2 L_g \frac{dI_1}{dt} \tag{10}$$

$$V_2 = L_c \frac{dI_2}{dt} + \frac{N_1}{N_2} L_c \frac{dI_1}{dt} + \frac{N_2}{N_7} L_g \frac{dI_2}{dt} + (\frac{N_2}{N_7})^2 L_g \frac{dI_2}{dt} \tag{11}$$

$$V_3 = L_g\frac{dI_2}{dt} - \frac{N_1}{N_7}L_g\frac{dI_1}{dt} + L_g\frac{dI_2}{dt} + \frac{N_2}{N_7}L_g\frac{dI_2}{dt} \tag{12}$$

where $L_c = \frac{N_2^2}{2R_c}$, $L_g = \frac{N_7^2}{2R_g}$.
Figure 5 shows the circuit to realize Eqn. (10) through Eqn. (12). The circuit in figure 5 is the basic model of the dipole magnet with no consideration of copper and core loss and parasitic capacitance. The circuit needs to be further modeled. But, however, the circuit provides us with an idea where to look for the electrical circuit configuration.

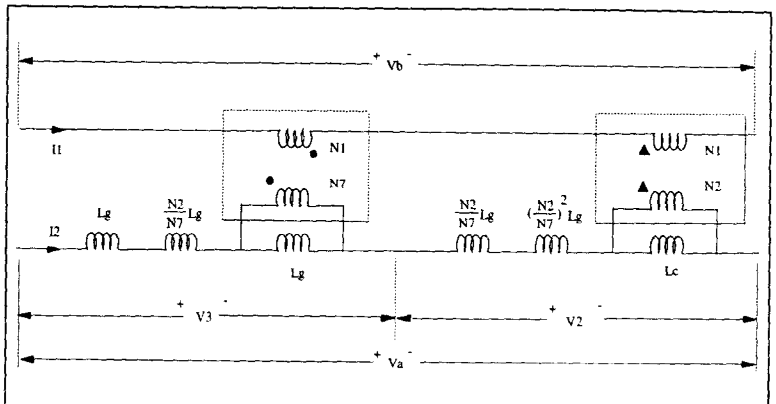

Fig 5. Equivalent Electrical Circuit From Magnetic Circuit

3.2 10 KHz Electrical Models

Based on the impedance matrix measurement and the basic circuit model in figure 5, A five-terminal electrical model can be curve fitted into its impedance matrix by using circuit simulation program Spice.

The DC resistance of the dipole buses are measured and scaled up to the resistance at 40°C. This resistance represents the copper loss of the magnet.

The through bus impedance is measured by Z_{11}, Z_{33}, Z_{13}, and Z_{31} in the impedance matrix measurement. Notice that Z_{11} and Z_{33} are same in both magnitude and phase. Z_{11} and Z_{13} are same in magnitude but 180° out of phase because of the reversed current. This implies that the through bus is symmetrical since the impedance looking into both terminals of the through bus is equal. The Z_{11}, Z_{33}, Z_{13}, and Z_{31} measurements reflect there is external wire resistance (8 mΩ) at each terminal.

The coil bus impedance is measured by Z_{22}, Z_{44}, Z_{24}, and Z_{42} in the impedance matrix. Notice that Z_{22} and Z_{44} are same in both magnitude and phase. Z_{22} and Z_{24} are same in magnitude but 180° out of phase due to the reversed direction of the current. This implies that the coil bus is symmetrical (at least to 10 KHz) since the impedance looking into both terminals of the coil bus is equal.

Coupling between buses is measured by Z_{21}, Z_{41}, Z_{12}, Z_{32}, Z_{23}, Z_{43}, Z_{14}, and Z_{34} in the impedance matrix. The Z_{12}, Z_{21}, Z_{34}, Z_{43} are equal and Z_{14}, Z_{41}, Z_{32}, Z_{23} are essentially the same. Z_{21} and Z_{14} are the same in magnitude but 180° out of phase.

The bus capacitance is measured by Z_{15}, Z_{25}, Z_{35}, Z_{45}, Z_{55}, Z_{51}, Z_{52}, Z_{53}, and Z_{54}. The Z_{55} measurement gives information of total capacitance from bus to ground. Z_{15} and Z_{51} measure the lumped capacitance from terminal 1 to ground while other terminals are grounded. Z_{52} and Z_{25} measure the lumped capacitance from terminal 2 to ground while other terminals are grounded. Z_{53} and Z_{35} measure the lumped capacitance from terminal 3 to ground while other terminals are grounded. Z_{54} and Z_{45} measure the lumped capacitance from terminal 4 to ground while other terminals are grounded. The Z_{51} and Z_{53} measurements are no available because the nearly zero volt excitation voltage V_1 and V_3 due to the current output limitation of the frequency generator.

Fig 6 shows the 6-meter and 4-meter dipole 10KHz electrical models. The models are obtained based on the impedance matrix measurement. The measurement data and the model simulation results are given in appendix A for 6-meter dipole and appendix B for 4-meter dipole. The models are well matched the impedance matrix for the frequency to 10KHz. The models have no significant difference on the impedance matrix measurement for the Armco and LTV steel magnets.

3.3 Simplified Electrical Models

The 10 KHz models shown in figure 6 are complicated especially when 344 magnets are connected together in SPICE simulation. It will take a lots of computer RAM memories and CPU time for each simulation. The measurement models therefore need to be simplified but yet keep the electrical characteristics of the dipole magnets. The dipole ring magnets will be connected in the way that the through bus of next magnet connecting with the coil bus of the previous magnet. The B magnet and A magnet are 6 meter dipole with coil bus and through bus position exchanged. Similarly, C and D magnet are the 4 meter dipole with coil bus and through bus position exchanged. The inductive coupling becomes less effect when the magnets are connected in series. Figure 7 shows the simplified model for 6 meter and 4 meter dipole magnet. The comparison between 10 KHz and simplified models are shown in figure 8 and 9 for two six-meter magnet string differential input impedance and common mode input impedance. Both impedance simulations are well matched for the frequency to 100 KHz. Similar result is obtained for two four-meter dipole magnet string.

Work has been done on application of the dipole electrical models on a eight-dipole magnet string. This dipole string is connected in the dipole configuration of B-A-B-A-D-C-B-C. Figure 10 shows the magnet string differential input impedance and Fig 11 shows the magnet string common mode input impedance from measurement, 10KHz models, and simplified models. The results state that the simplified models are accurate.

4. Conclusion

Impedance measurement shows no significant difference between Armco and LTV steel dipole magnets. The simplified electrical models can be used as a sub circuit to build the main injector dipole ring Spice model to study the frequency and transient behaviors of the system.

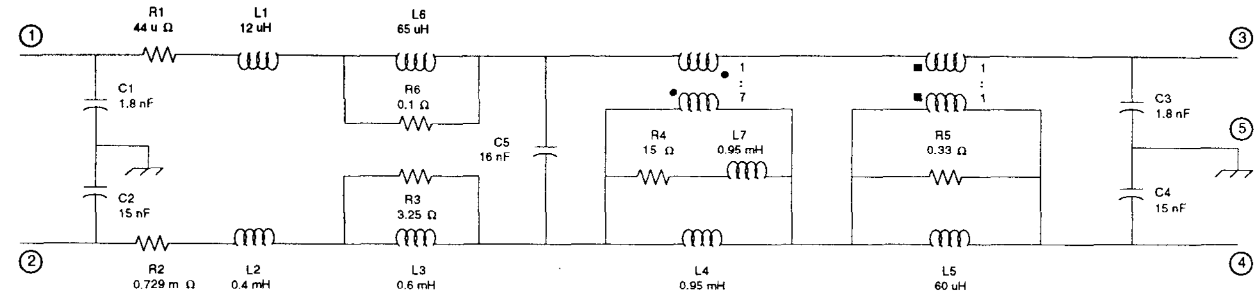

(a) Main Injector 6-Meter Dipole Magnet 10 KHz Electrical Model

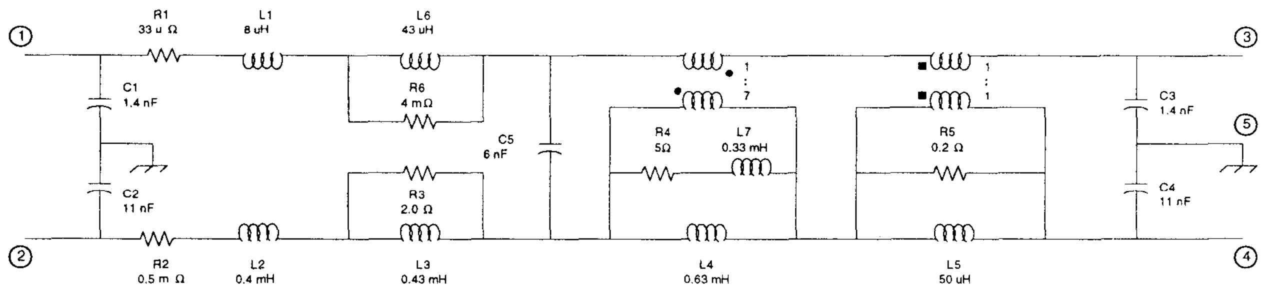

(b) Main Injector 4-Meter Dipole Magnet 10 KHz Electrical Model

Fig 6. Main Injector Dipole Magnet 10 KHz Electrical Models (a) 6 Meter (b) 4 Meter

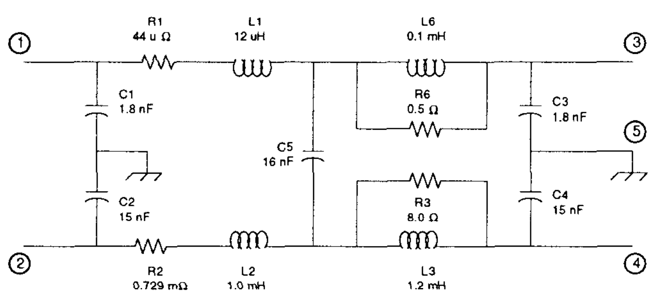

(a) Main Injector 6-Meter Dipole Magnet Simplified Electrical Model

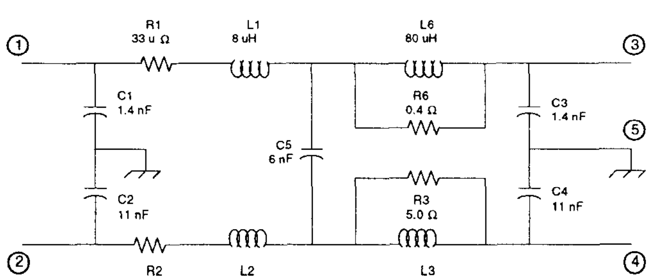

(b) Main Injector 4-Meter Dipole Magnet Simplified Electrical Model

Fig 7. Main Injector Dipole Magnet Simplified Electrical Models (a) 6 Meter (b) 4 Meter

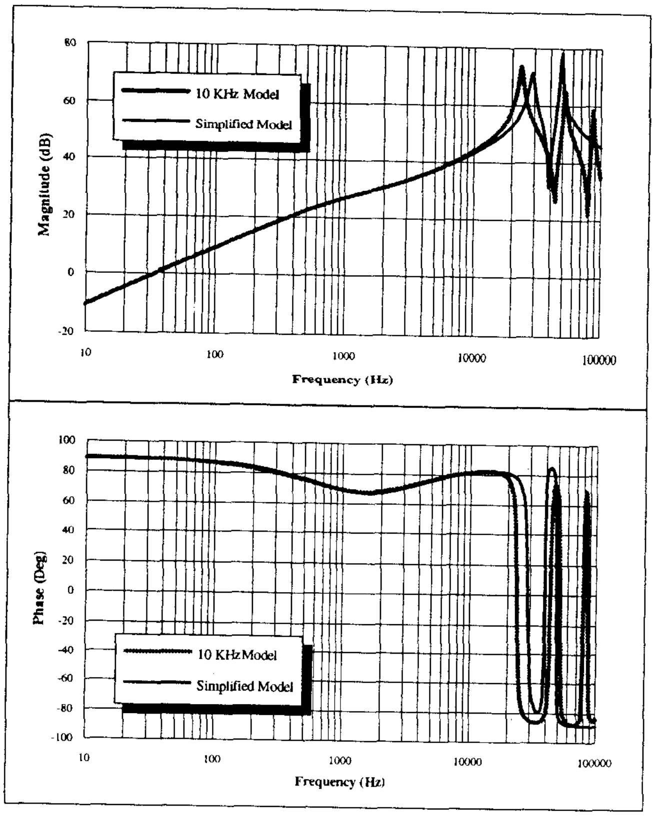

Fig 8 Two 6-Meter Dipole String Differential Input Impedance

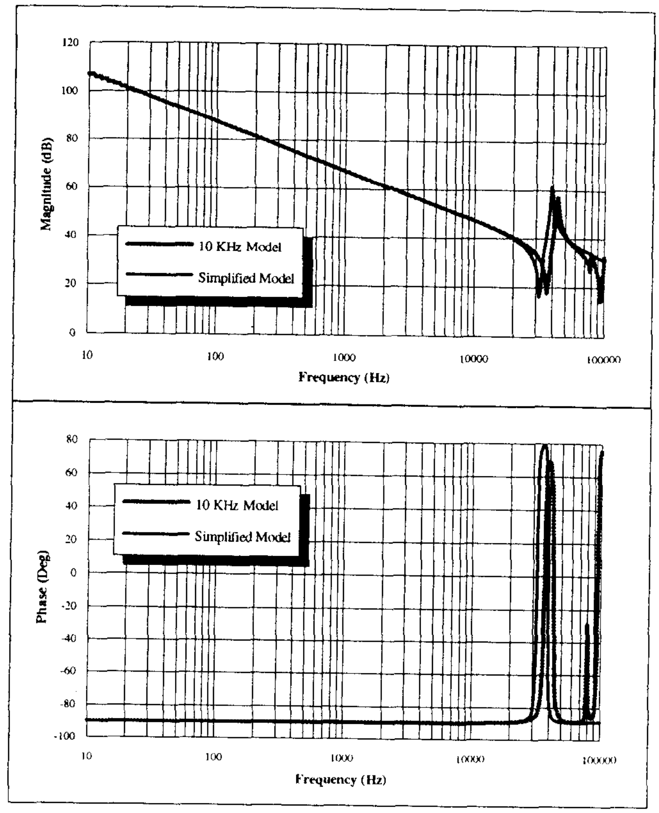

Fig 9 Two 6-Meter Dipole String Common Mode Input Impedance

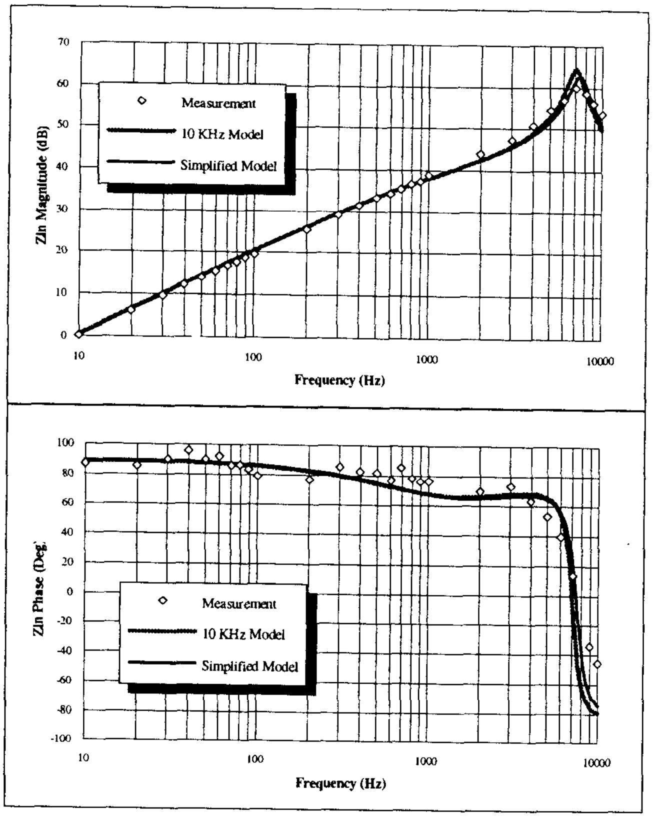

Fig 10 8 Dipole Magnets String Differential Input Impedance

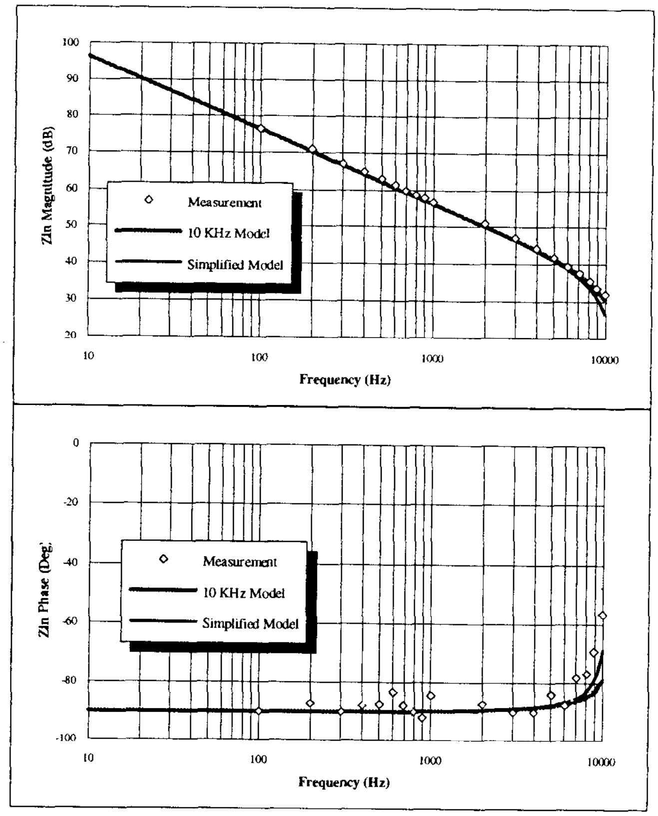

Fig 11 8 Dipole Magnet String Common Mode Input Impedance